Appl. Phys. B 48, 293–297 (1989)

Applied Physics B Photophysics and Laser Chemistry

Multiple Harmonic Conversion of Pulsed CO_2 Laser Radiation in Tl_3AsSe_3

R. C. Y. Auyeung*, D. M. Zielke, and B. J. Feldman

Laser Physics Branch, Naval Research Laboratory, Washington, DC 20375-5000, USA

Received 1 February 1988/Accepted 30 November 1988

Abstract. The nonlinear material Tl_3AsSe_3 is used to convert pulsed 9.6 μm CO_2 laser radiation into its second, third, fourth and fifth harmonic. Internal (external) conversion efficiencies of 28, 14(6.7), 3.6(3.1), and 0.5(0.3)% from the pump fundamental are achieved in 4.8, 3.2, 2.4, and 1.9 μm generation respectively.

PACS: 42.65.Cq, 42.70, 42.55.Dk

There remains a need for a powerful and tunable coherent radiation source in the near- to mid-infrared region. Currently, radiation in this region is provided by sources such as HF, DF, CO, and CO_2 lasers. An attractive method of generating new IR sources is frequency conversion in nonlinear materials. In this paper we present results of various frequency conversion processes in the nonlinear material Tl_3AsSe_3 (TAS) using a pulsed CO_2 laser. The conversion of CO_2 laser radiation into its second through fifth harmonic is reported.

In the past, nonlinear frequency conversion in the infrared has met with limited success due to the difficulty in obtaining high-quality nonlinear materials. However, recent improvements in the growth of nonlinear materials such as $AgGaSe_2$, $CdGeAs_2$, and $ZnGeP_2$ have led to renewed interest in this area. Efficient second harmonic conversion and optical parametric oscillation (OPO) have been demonstrated in $AgGaSe_2$ [1, 2], while second harmonic generation (SHG) has been performed in $CdGeAs_2$ [3] and $ZnGeP_2$ [4]. At present all of these materials are limited to sizes of ~1–2 cm in length and ~1 cm^2 in cross-section.

Thallium arsenic selenide (TAS), a member of the ternary chalcogenide salts, is another attractive material for nonlinear frequency conversion in the infrared. This negative uniaxial crystal was originally grown in 1972 at Westinghouse Research Laboratories using the Bridgman technique [5]. Second harmonic generation of CO_2 laser radiation and measurements of various crystal parameters were performed on these early samples of TAS which were ~1.2 cm in diameter and 3 cm in length. Since the first synthesis of this material, many studies have been made on the properties of TAS which are important in nonlinear frequency conversion. These studies have shown that TAS has a wide transparency range (1.3–17 μm) [6], low absorption/scattering coefficient ($\lesssim$0.5 %/cm) [6], relatively large nonlinear coefficient ($d_{\text{eff}} = (66 \pm 30\%) \times 10^{-12}$ m/V) [5, 7], moderate damage threshold (1.5 J/cm^2) [8] and is readily grown to large crystal sizes ($2.5 \times 2.5 \times 10\,cm^3$). Its refractive indices have been accurately measured [9] and have led to calculated phase-matched angles in good agreement with experiment. Some previous work on frequency conversion in TAS has been performed by using this material as an intracavity doubler in a TEA CO_2 laser [10].

We have recently received from Westinghouse R & D Center several good-quality large (2.5 cm dia. × 6 cm) TAS samples. In the present series of experiments, TAS is used to frequency double pulsed CO_2 laser radiation at 9.6 μm, double 4.8 μm radiation to 2.4 μm and convert the CO_2-fundamental into 3.2 μm and 1.9 μm radiation by frequency mixing the various harmonics. These preliminary results demonstrate that TAS can considerably extend the wavelength range of the CO_2 laser and is a promising candidate for a powerful and tunable source throughout the infrared.

* Geo-Centers Inc., Fort Washington, MD 20744, USA

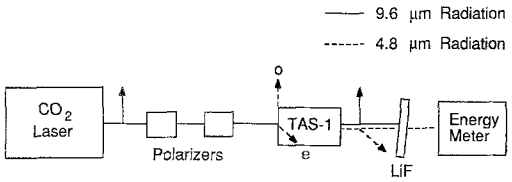

Fig. 1. Schematic diagram of the apparatus used for second harmonic generation (SHG). The polarizers are used to attenuate the 9.6 μm pump beam. The LiF filter is 93% transmitting at 4.8 μm and totally opaque at 9.6 μm. The arrowed lines indicate the polarization of the various harmonics

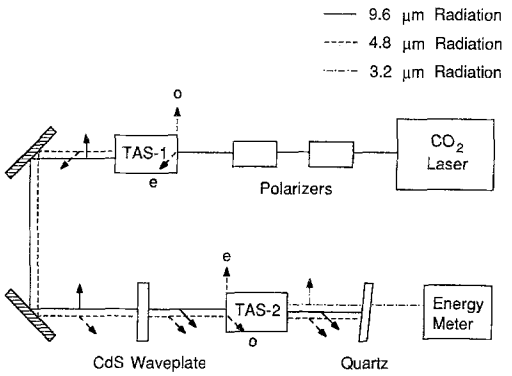

Fig. 2. Schematic diagram of the apparatus used for frequency tripling. The CdS waveplate is $7\lambda/2$ at 9.6 μm, 8λ at 4.8 μm and AR-coated at both wavelengths. The quartz filter is 83% transmitting at 3.2 μm and totally opaque above 4.5 μm. Coating losses of TAS-2 and its windows result in a crystal transmission of 23% at 3.2 μm

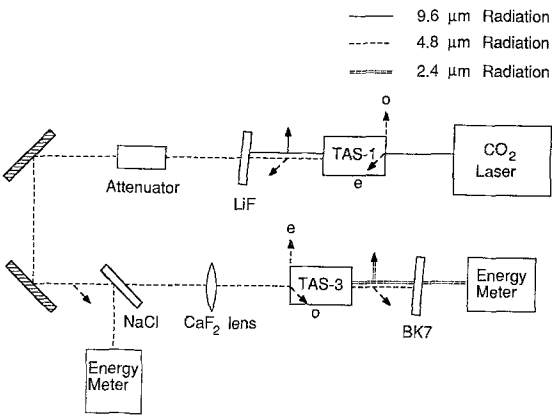

Fig. 3. Schematic diagram of the apparatus used in doubling the second harmonic. Coating losses of TAS-3 and its windows result in a crystal transmission of 88% and 84% at 4.8 and 2.4 μm respectively. The BK 7 filter is 88% transmitting at 2.4 μm and totally opaque above 4.5 μm

1. Experimental Procedure

The pump laser is a double-module Lumonics 822 HP (TEA) CO_2 laser operating at 0.5 Hz in the TEM_{00} mode but in multi-longitudinal mode. Optimized for frequency conversion experiments, the laser produced

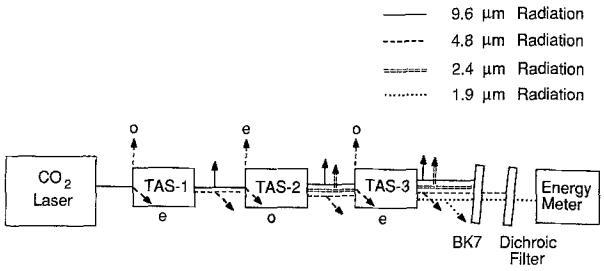

Fig. 4. Schematic diagram of the apparatus used in generating the fifth harmonic. Due to coating losses, the crystals TAS-2 is 30% transmitting at 2.4 μm and TAS-3 is 35% transmitting at 1.9 μm. The transmissions of the BK 7 and dichroic filters at 1.9 μm are 92% and 67% respectively

~300 mJ of linearly polarized output in a ~70 ns FWHM pulse (without a nitrogen tail) on the 9.55 μm P(20) transition. The beam area at the $1/e^2$ intensity points was 0.8 cm^2.

For SHG experiments with the CO_2-fundamental, two TAS crystals designated as TAS-1 and TAS-2 were grown with the angle between the optic axis and the boule axis at ~19°. For SHG with the doubled CO_2-fundamental, a third crystal designated as TAS-3 was grown with the angle at ~28°. All crystals are grown with the boule axis positioned in the $b-c$ plane. Typical dimensions of the crystals used in this work are 2.5 cm in diameter and 5–6 cm in length. Each of the TAS crystals is mounted in a hermetically sealed aluminum cylinder. The end surfaces of the crystal are AR-coated due to the high index of refraction of TAS (~3.3). Because these coatings are hygroscopic, ZnSe windows with non-hygroscopic AR coatings are used to protect the end surfaces. The AR-coatings in the crystals TAS-1 and TAS-2 are designed at 9.6 and 4.8 μm, and in TAS-3, at 4.8 and 2.4 μm.

The energies of the laser fundamental and lower harmonics are measured on a Gentec ED-500 pyroelectric detector while a more sensitive Gentec ED-200 detector is used to record the fourth and fifth harmonic energies. In all cases, the total energy is measured; no apertures are used in front of the detectors. The temporal pulse shapes are recorded on a fast Hg : Cd : Te detector (risetime ~4 ns).

All frequency mixing experiments are performed under Type I conditions. Figures 1–4 show schematic diagrams of the apparatus used in generating the various harmonics. The even harmonics are produced by second harmonic generation and the odd harmonics, by sum frequency conversion.

2. Results

The nonlinear properties of TAS were examined by measuring the conversion efficiency and the harmonic

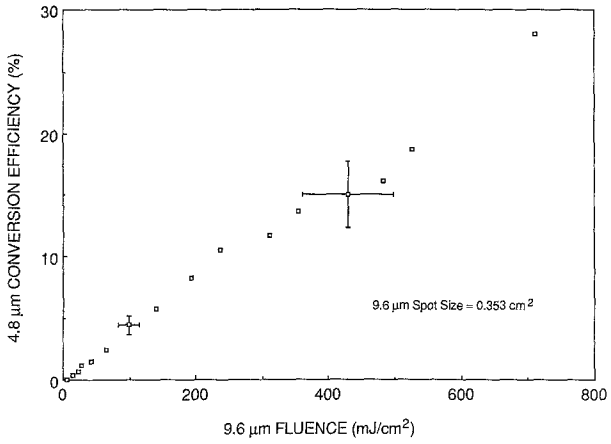

Fig. 5. Variation of the second harmonic energy conversion efficiency as a function of 9.6 μm pump fluence. The spot size contains ~50% of the total 9.6 μm energy

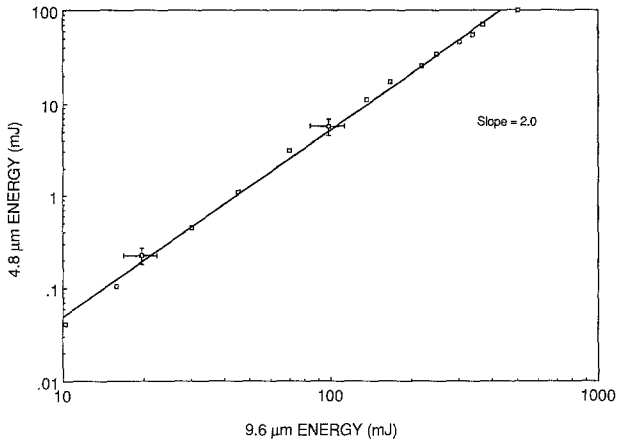

Fig. 6. Variation of the 4.8 μm energy as a function of 9.6 μm pump energy

output as a function of pump energy. All plotted fluences and energies refer to values inside the crystal and both are directly proportional to the peak intensity. Coating losses in the crystal ends and windows are determined from transmission measurements of the laser fundamental and harmonics. Except for the 3.2 μm and 1.9 μm generation experiments, the correction factor between external and internal energies is $<10\%$.

Figure 5 is a graph of the second harmonic conversion efficiency with respect to the CO_2 laser fluence. An overall conversion efficiency of 28% from the fundamental was measured in TAS-1 at an incident fluence of $\sim 700\,mJ/cm^2$ near the expected phase-matched angle of ~19°. This conversion efficiency represents the highest second harmonic conversion of the CO_2-fundamental reported to date. The 4.8 μm pulse (~40 ns FWHM) displays rapid temporal modulation in similarity to the behaviour in the fundamental pulse. A log–log plot of the second harmonic energy with respect to the fundamental energy is shown in Fig. 6. A least-squares-fit through the data produces a slope of 2.0 in excellent agreement with theory.

The third harmonic of the CO_2-fundamental is generated by sum frequency conversion in a second crystal, TAS-2, tuned close to the phase-matched angle of ~21°. In order to perform Type I tripling, a $7\lambda/2$ (at 9.6 μm) CdS waveplate is used to rotate the 9.6 μm polarization by 90°. The waveplate acts as an 8λ or fullwave plate at 4.8 μm thus leaving the 4.8 μm polarization unchanged. Figure 7 is a graph of the 3.2 μm energy conversion efficiency with respect to the pump fluence. The external efficiency corrects for losses at the quartz filter whereas the internal efficiency includes the coating losses of TAS-2 at 3.2 μm. At incident 9.6 μm and 4.8 μm fluences of $\sim 310\,mJ/cm^2$ and $\sim 100\,mJ/cm^2$ respectively, an external (internal)

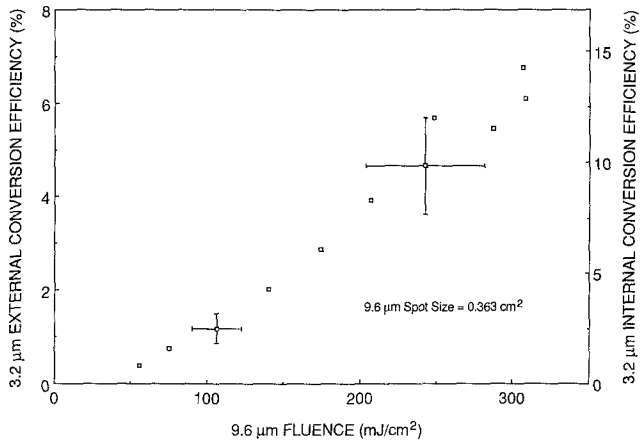

Fig. 7. Variation of the 3.2 μm energy conversion efficiency (with respect to the fundamental) as a function of 9.6 μm fluence. The spot size contains ~50% of the total 9.6 μm energy

conversion of 6.7%(14%) from the fundamental was measured. A log–log plot of the 3.2 μm energy with that of the fundamental is shown in Fig. 8. A least-squares-fit through the data produces a slope of 2.6 which is lower than the anticipated value of 3. This discrepancy is probably due to crystal inhomogeneity and poor 4.8 μm beam quality.

The fourth harmonic of the CO_2-fundamental is generated by doubling the second harmonic in another TAS crystal, TAS-3, tuned close to the Type I phase-matched angle of ~27°. Because in preliminary experiments no evidence of damage was observed in TAS-3 with the 4.8 μm output from TAS-1, a CaF_2 lens (50 cm focal length) was placed ~26 cm from TAS-3 to obtain a higher 4.8 μm pump fluence. A plot of the 2.4 μm conversion efficiency with respect to the second harmonic fluence is shown in Fig. 9. The external efficiency corrects for losses at the BK 7 filter and the

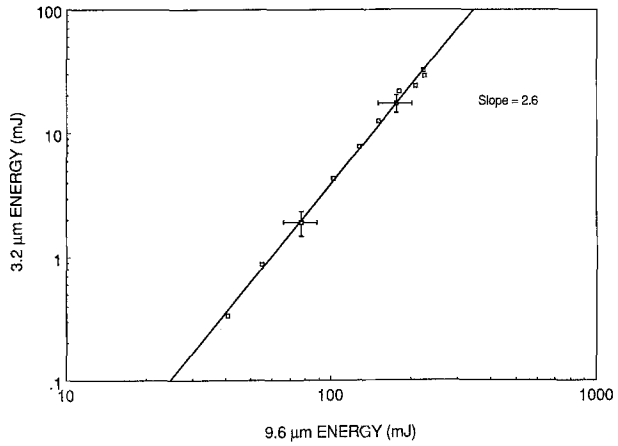

Fig. 8. Variation of the third harmonic energy as a function of the 9.6 μm pump energy

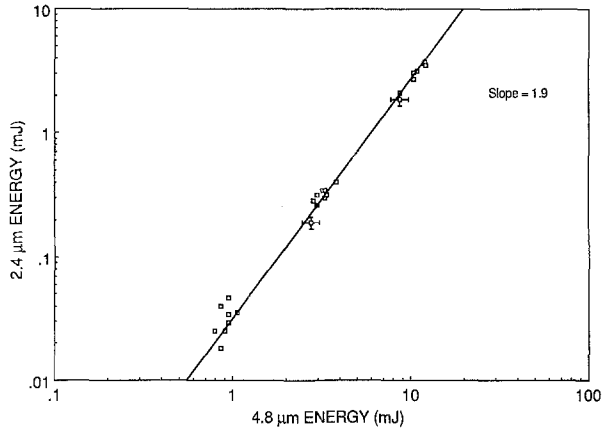

Fig. 10. Variation of 2.4 μm energy as a function of 4.8 μm energy

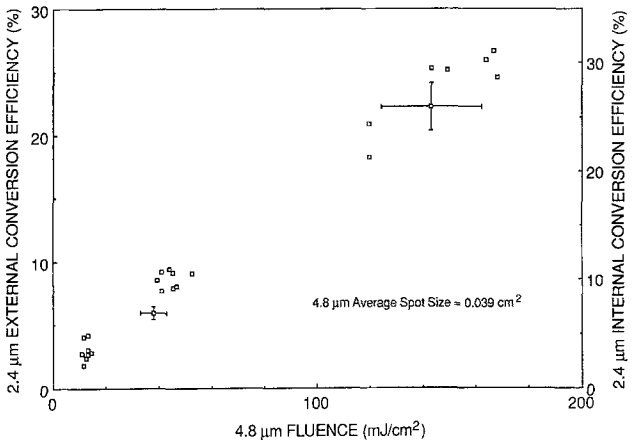

Fig. 9. Variation of the 2.4 μm energy conversion efficiency (with respect to the second harmonic) as a function of 4.8 μm pump fluence. The spot size contains ~50% of the total 4.8 μm energy and represents the value at the center of the crystal

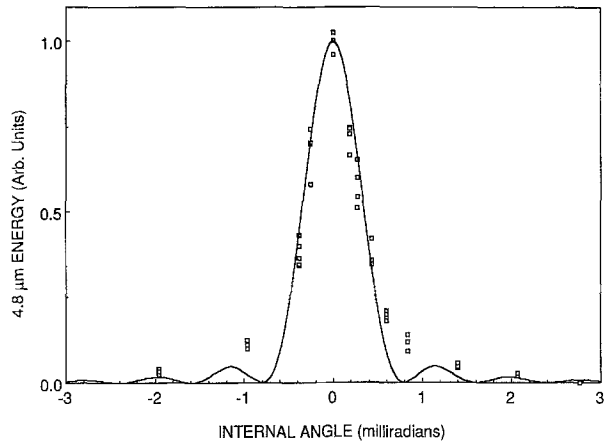

Fig. 11. Phase-matching tuning curve for SHG in TAS-1. The solid line is the calculated curve for a crystal length of 5 cm

internal efficiency includes the coating losses of TAS-3 at 4.8 μm and 2.4 μm. The 4.8 μm spot size is an average of the entrance and exit beam areas and was measured without the crystal in place. At an incident 4.8 μm fluence of ~170 mJ/cm^2, an external (internal) conversion efficiency of ~27%(31%) was measured. It is interesting to note that since the conversion efficiency varies as $1/\lambda^2$ [11], the same efficiency can be achieved in doubling the second harmonic as can be attained in doubling the fundamental but with one-quarter the pump fluence. In general then, high conversion efficiencies should be easier to achieve with shorter pump wavelengths. A log–log plot of the 2.4 μm energy with the second harmonic energy is shown in Fig. 10. A least-squares-fit through the data results in a slope of 1.9 in very good agreement with theory.

Encouraged by the high fourth harmonic conversions, we used the same crystal TAS-3 to generate the fifth harmonic by summing the fundamental and the fourth harmonic at the Type I phase-matched angle of ~28°. In this case, the fourth harmonic was produced by tilting the crystal TAS-2 ~27° from normal incidence since this crystal was originally cut for SHG at a phase-matched angle of ~19°. At internal 9.6 μm and 2.4 μm fluences of 190 and 12 mJ/cm^2 respectively, ~0.4 mJ of 1.9 μm output was obtained correcting only for losses at the filters. If the losses at the AR coatings on the crystal are included, the estimated internal 1.9 μm energy would be ~0.7 mJ which corresponds to an internal conversion efficiency of 45% from the fourth harmonic or 0.5% from the fundamental. The 1.9 μm internal conversion efficiency was further confirmed by examining the 2.4 μm energy in the presence and absence of the 9.6 μm pump beam. A decrease of ~43% in the 2.4 μm signal was observed when the 9.6 μm pump beam was unblocked, in good

agreement with the above value of internal conversion from the fourth harmonic to the fifth. A major limitation in 1.9 μm conversion efficiency was the angular separation of the fundamental and the fourth harmonic output from TAS-2 caused by the steep crystal angle used in 2.4 μm generation.

The optical quality of the TAS crystals was further investigated by performing a phase-matching tuning curve in TAS-1 as shown in Fig. 11. The 5-cm interaction length deduced from curve-fitting the data is ~80% of the actual crystal length and is indicative of relatively good crystal quality.

The nonlinear coefficient d_{eff} is one of the most important parameters of a nonlinear material and it can be easily extracted from log–log plots of the second harmonic energy with respect to the pump energy. Although the experiments in this work are not designed for a very accurate determination of d_{eff} due to temporal structure in the laser pulse, the deduced values should still prove useful in crystal evaluation. Under phase-matched conditions and in the absence of pump depletion, the energy of the second harmonic E_S may be approximated in terms of the fundamental energy E_F by the expression,

$$E_S = GL^2(T_S/T_F^2)(R_S/R_F^2)E_F^2, \quad (1)$$

where $G = 2\omega^2 d_{eff}^2/(\varepsilon_0 n^3 c^3)$, L is the crystal interaction length and $T_{F,S}$ and $R_{F,S}$ are the integrated temporal and spatial distributions for the fundamental and second harmonic. From Fig. 6, the deduced y-intercept results in a calculated d_{eff} of $\sim 19 \times 10^{-12}$ m/V. The spatial beam profiles are assumed to be Gaussian for this calculation. In another experiment with a shorter 2.2 cm-long TAS crystal, a direct comparison of the second harmonic conversion of this crystal with that of TAS-1 results in a deduced d_{eff} of $\sim 29 \times 10^{-12}$ m/V which is within a factor of two of previous reported measurements.

3. Conclusions

In this work, TAS has been used to convert the 9.6 μm output of a pulsed CO_2 laser into its second, third, fourth and fifth harmonic. A summary of the measured internal and external conversion efficiencies is shown in Table 1. Although the generated harmonics do not completely cover the near- to mid-IR region, the 9–11 μm wavelength range of the CO_2 laser ensures that a band of tunability is available at each harmonic.

Table 1. Summary of measured internal and external energy conversion efficiencies with respect to the 9.6 μm CO_2-fundamental. The pump fluences represent the actual energy deposited into the crystal

Harmonic	Internal (%)	External (%)	Internal fluence (mJ/cm²)
2ω	28	28	λ(9.6 μm) = 700
3ω	14	6.7	λ(9.6 μm) = 310 λ(4.8 μm) = 100
4ω	3.6	3.1	λ(4.8 μm) = 170
5ω	0.5	0.3	λ(9.6 μm) = 190 λ(2.4 μm) = 12

The measured conversion efficiencies in this work demonstrate the strong potential of TAS to extend the wavelength coverage of coherent sources throughout the IR. Work in improving the purity, homogeneity and coatings of these crystals is in progress and should eventually lead to further advancements in crystal performance.

Acknowledgements. The TAS crystals used in this work were grown by Westinghouse R & D Center for the Naval Research Laboratory under contract N 00014-86-C 2152. We are grateful to T. Henningsen and his coworkers at Westinghouse for numerous technical discussions regarding TAS. Suppport for this work was provided by DARPA and the Navy SPAWAR office.

References

1. R.C. Eckardt et al.: Appl. Phys. Lett. **47**, 786 (1985)
2. R.C. Eckardt et al.: Appl. Phys. Lett. **49**, 608 (1986)
3. Yu.M. Andreev et al.: Sov. J. Quant. Electron. **17**, 491 (1987)
4. Yu.M. Andreev et al.: Sov. J. Quant. Electron. **15**, 1014 (1985)
5. J.D. Feichtner, G.W. Roland: Appl. Opt. **11**, 993 (1972)
6. K.K. Deb, R.E. Longshore: Mat. Res. Bull. **20**, 281 (1985)
7. R.L. Byer, R.L. Herbst: Parametric Oscillation and Mixing, in *Nonlinear Infrared Generation*, ed. by Y.-R. Shen, Topics Appl. Phys., Vol. 16 (Springer, Berlin, Heidelberg 1977) p. 81
8. H. Kildal, G.W. Iseler: Appl. Opt. **15**, 3062 (1976)
9. M.D. Ewbank et al.: J. Appl. Phys. **51**, 3848 (1980)
10. R.L. Pastel: Appl. Opt. **26**, 1574 (1987)
11. A. Yariv: *Introduction to Optical Electronics*, 2nd ed. (Holt, Rinehart and Winston, New York 1971) p. 211